Manuscript refereed by Dr Marco Actis Grande, Politecnico di Torino

Scalmalloy® = A Unique High Strength AlMgSc Type Material Concept Processed by Innovative Technologies for Aerospace Applications

Frank Palm[1], Ronny Leuschner[2], Thomas Schubert[2], Bernd Kieback[2],
[1] EADS Innovation Works, D-81663 Ottobrunn/München,
[2] Fraunhofer-Institut für Angewandte Materialforschung, D-01277 Dresden,

Abstract
Unconventional structures in materials may be generated by the corresponding choice of alloys in combination with a rapid extraction of heat. Improved melt spinning procedures allow to solute more than 1.0 wt% Sc in the Al-lattice. Therefore a critical cooling rate is necessary, which can only be achieved by ribbon thickness lower than 25 µm. In the next step, the flakes are usually compressed with high pressures and temperatures, whereby the fine microstructures may be damaged due to grain growth. However, that grain growth can be successfully suppressed by nano-scaled $Al_3(Sc_{1-x}; Zr_x)$ precipitations. Spark Plasma Sintering (SPS) is a short time sintering technique related to hot pressing, which uses a pulsed electrical current for the direct heating of the sinter body. The use of high heating rates and short dwell times can minimise grain growth, which often leads to improved material properties. Important technological benefits, such as the energy efficiency due to short processing time, fewer processing steps, elimination of the need for sintering aids, and near net shape capability, are possible.

Introduction

The use of lightweight construction material and the consistent utilisation of its properties for mass application are of major importance for numerous future developments and implementations in various fields in the automotive and aircraft industry. At AEROMAT2006 in Seattle a new engineering material concept basing on hypereutectically Sc alloyed AlMgMn was revealed. Its principle metallurgy originates from supersaturation of the AlMg matrix with Sc and Zr which requires fast cooling procedures during solidification. Due to its very high aging response (0.1 wt% Sc can generate 50 MPa strength increase) “soft” Al-alloys like AlMg4.5Mn (AA5083) can be reinforced by more than 300 % in terms of yield strength without sacrificing their renowned manufacturing properties [1]. The patended Scalmalloy® sheet material manufacturing procedure differs significantly from “classically” rolled AlMgSc sheet materials known from Russia (i.e. RUS1570), Germany (ALERIS KO8242) or the US (ALCOA C557). As its strength is derived mostly from precipitation hardening via $Al_3(Sc_{1-x}; Zr_x)$ and not from strong cold rolling it can develop a unique combination of fracture toughness and high yield strength. Hence low cost and corrosion resistant airframe shell structures with very good properties might become feasible. But, “freezing” of more than 1.0 wt% Sc in the Al-lattice is very difficult [2, 3]. Besides the development of such high-performance materials itself, the economic processing into components is a stringent necessity to increase acceptance for a widespread practical implementation of the knowledge. The existing production chain of high-temperature resistant aluminium materials shows long processing intervals, particularly with the compaction of the powders into a semi-finished part. Conditional on the procedure, simultaneously elevated temperatures lead to unpreferred changes of the structure caused by grain growth and formation of intermetallic precipitations [4]. Furthermore, that makes the process of the following forming difficult and impairs the mechanical properties of the manufactured components made in such a way. The use of appropriate alloying elements can prevent grain growth, for example with scandium in aluminium alloys [5, 6]. However, the solubility of scandium in aluminium is limited to about 0.5 wt%. Though, having a sufficiently high solidification rate, the dissolution of 0.5-3 wt% Sc concentration in solid solution is

successful [7]. At the same time, the rapid solidification of the molten metal results in a very fine grain structure in micrometer size as well as in homogenous allocation of the alloy elements. At a following thermal treatment, the dissolved Sc in combination with Zr can form specifically coherent $Al_3(Sc_{1-x}; Zr_x)$-phases [8, 9]. Avoiding unwanted or irreparable precipitation reactions, in particular, coarsening of the $Al_3(Sc_{1-x}; Zr_x)$-phases, the temperature field has to be defined and restricted at the subsequent compaction and hot forming. Thus guaranteed high density of these nano-structured, homogeneously allocated and limited thermal substantial $Al_3(Sc_{1-x}; Zr_x)$-precipitations effect significant strengthening with high ductility [3].

Experimental

An Al Mg3.6Sc1.4Zr0.2Mn0.3 (specification in wt%) alloy was used as a base material for the rapid solidification. The production of the < 50 µm thick ribbons was carried out by pouring the molten metal with a temperature of 900 °C onto a water-cooled rotating copper wheel with a circumferential velocity variation between 25 and 45 m/s. Preventing oxidation of the molten metal and the ribbons during the quenching, an argon atmosphere was applied. For the following working steps the temperature-time-behaviour of the material was investigated. This heat treatment of the rapidly solidified flakes at 300, 325, and 350 °C and time periods ranging from 6 to 960 min result in the $Al_3(Sc_{1-x}; Zr_x)$-precipitation which are responsible for the increase in strength. Furthermore, the rapidly solidified ribbons were shredded by a chopper into about 1 mm flakes. Afterwards, the compaction was carried out by Spark Plasma Sintering into dense cylindrical blanks. The compaction method is characterised by a very short cycle time, to prevent long and high thermal stress for the material structure. All runs were executed in dynamic vacuum. The relative densities of the sintered specimens were determined by the Archimedes method. The samples were analysed after the several production steps. For that purpose, cross-sections for SEM micrographs were prepared and the formed precipitation could be verified element-specific by energy-dispersive X-ray analysis. In addition, the microhardness of the structure was measured and optical microscopy was performed after etching in Dix-Keller´s agent. Additionally, TEM images were used to determine the presence of $Al_3(Sc_{1-x}; Zr_x)$-precipitation after the heat treatment. The determination of the hydrogen content was carried out by hot gas extraction with a LECO TCH600.

Results and Discussion

Micro Hardness

A high cooling rate at melt spinning causes the forced dissolution of higher Sc and Zr concentrations in the aluminium and suppresses the $Al_3(Sc_{1-x}; Zr_x)$-phase formation. As a consequence, a successful forced dissolution of the alloy elements leads to a lower microhardness of the rapidly solidified structure. Figure 1a shows the measurable correlation between the ribbon thickness and the microhardness of the rapidly solidified alloy. The lower the ribbon thickness, the lower the micro hardness is. The lowest values from 120 to 135 HV are measured having ribbon thicknesses of about 20-25 µm. As ribbon thicknesses increase, the hardness values go up to 175 HV.

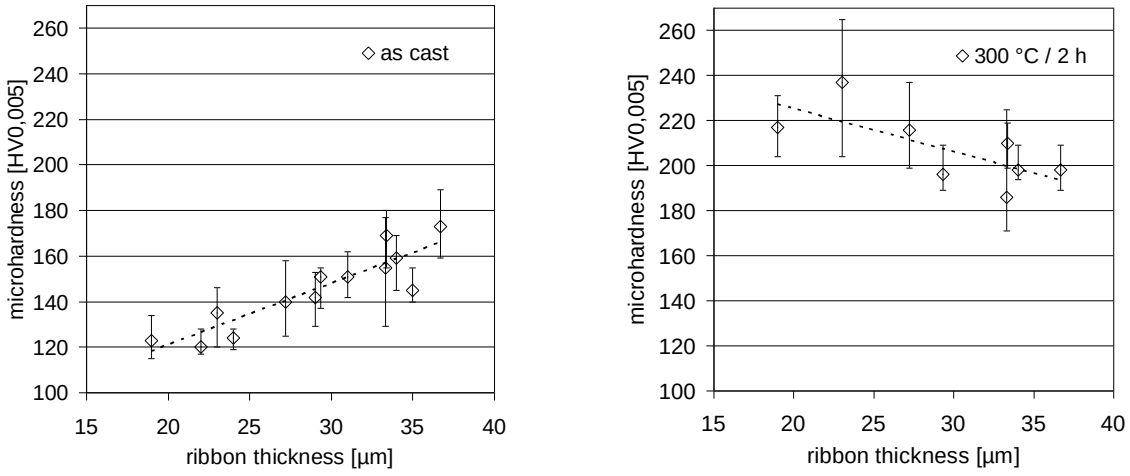

a) b)

Figure 1: Micro hardness values of rapidly solidified (a) and heat treated (b) samples. Increasing ribbon thickness causes a decreasing cooling rate and reduced solubility of Sc and Zr in the Aluminium (a).

A following thermal treatment is aimed to precipitate specifically of the forced dissolved Sc in combination with Zr as a secondary $Al_3(Sc_{1-x}; Zr_x)$-phase. So, a heat treatment of the rapidly solidified material was carried out in a series of tests for 2 h at 300°C. The results of the hardness measurements are summarised in figure 1b. The thinner the ribbons, the higher hardness values are measurable. After the heat treatment, those samples with the lowest hardness after solidification have the highest absolute values of up to 240 HV. This means an increase in hardness of more than 100 HV which refers to the precipitation of the secondary Al_3 $(Sc_{1-x}; Zr_x)$-phase. By contrast, only hardnesses between 190 and 210 HV can be measured with the thicker ribbons of 30-35 µm, which indicates an increase of about 25-45 HV compared to the rapidly solidified condition. Based on these results, only ribbon thicknesses < 30 µm were applied for the following tests to achieve maximum hardness. Previous studies with the reference material hardness measurements showed values of 200 HV combined with an ultimate tensile strength of 630 MPa for the extruded material. Therefore, values of about 220-240 HV a capability of 680-720 MPa UTS would be possible [3].

Varying of the heat treatment parameter, both, the temperature (300, 325 and 350°C) and the time period (6 min to 16 h), the limits of the following process steps are to be obtained. In figure 2, the overview of the measured microhardness of the melt-spun ribbons after the heat treatment indicates lower values in total for the annealing temperature of 350°C compared to 325 and 300°C. As the temperature increases, the particular maximum hardness emerge at an earlier stage. In detail, the maximum hardness 220 HV are reached at 300°C after 2 h, 215 HV at 325°C after 30 min and 205 HV at 350°C after 15 min. According to that, the temperature level and the length of time have influence on the formation of the precipitations.

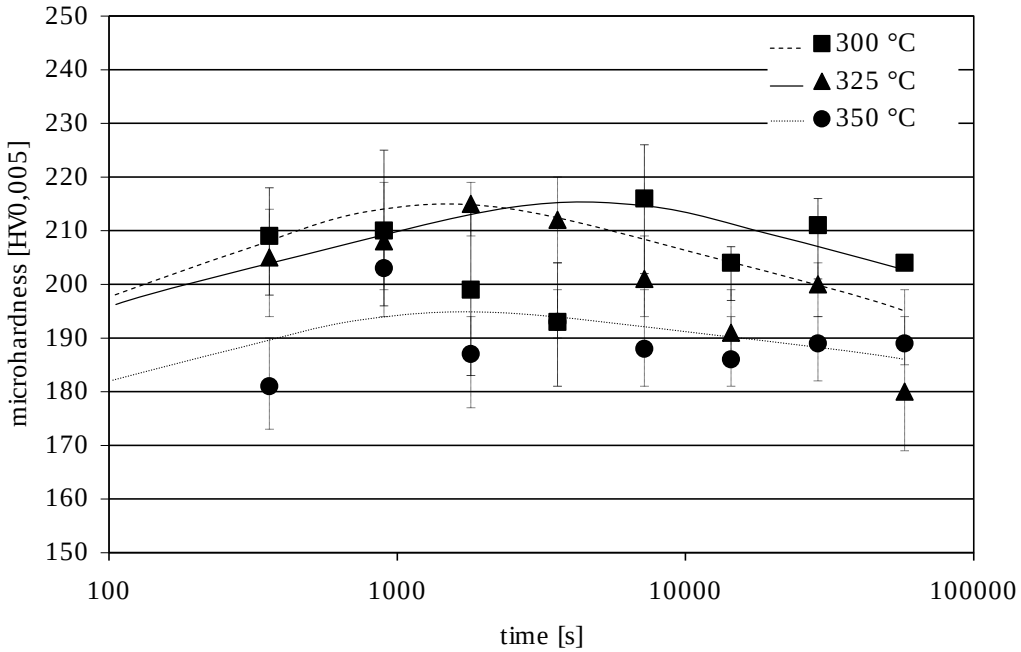

Figure 2: Micro hardness measurements after heat treatment at 300, 325 and 350°C for 6 min to 16 h of the rapidly quenched alloy with thickness < 35 µm.

Microstructure

Structure images of two rapidly solidified ribbons in a longitudinal section produced by a light and scanning electron microscope are shown in figure 3. The taken SEM images 3a and b of backscatter electrons, the mass differences of Sc and Zr to Al and their allocation can be depicted. Homogeneity can be seen in the thinner ribbon on the left side. In contrast, light spots on the top ribbon side are visible on the right. Sc and Zr can be verified in these bright areas by EDX analysis (not shown). In the left image below, lamellar grains are identifiable all over the entire ribbon thickness in etched condition. Two different structures occur in the right image below which separates the ribbon horizontally. In the lower area, on the wheel side, lamellar grains appear, whereas on the upper side of the ribbon globular ones. The cooling rate in the upper ribbon area is lower the on the wheel side. Obviously, increasing ribbon thickness reduces the cooling rate so far that it creates a globular microstructure. At the same time, the cooling rate is not adequate anymore to dissolve Sc and Zr in the aluminium. Thus, the bright areas in the SEM image present $Al_3(Sc_{1-x}; Zr_x)$-precipitations. These partial ribbon precipitations explain the higher hardness values at increasing ribbon thickness in figure 2.

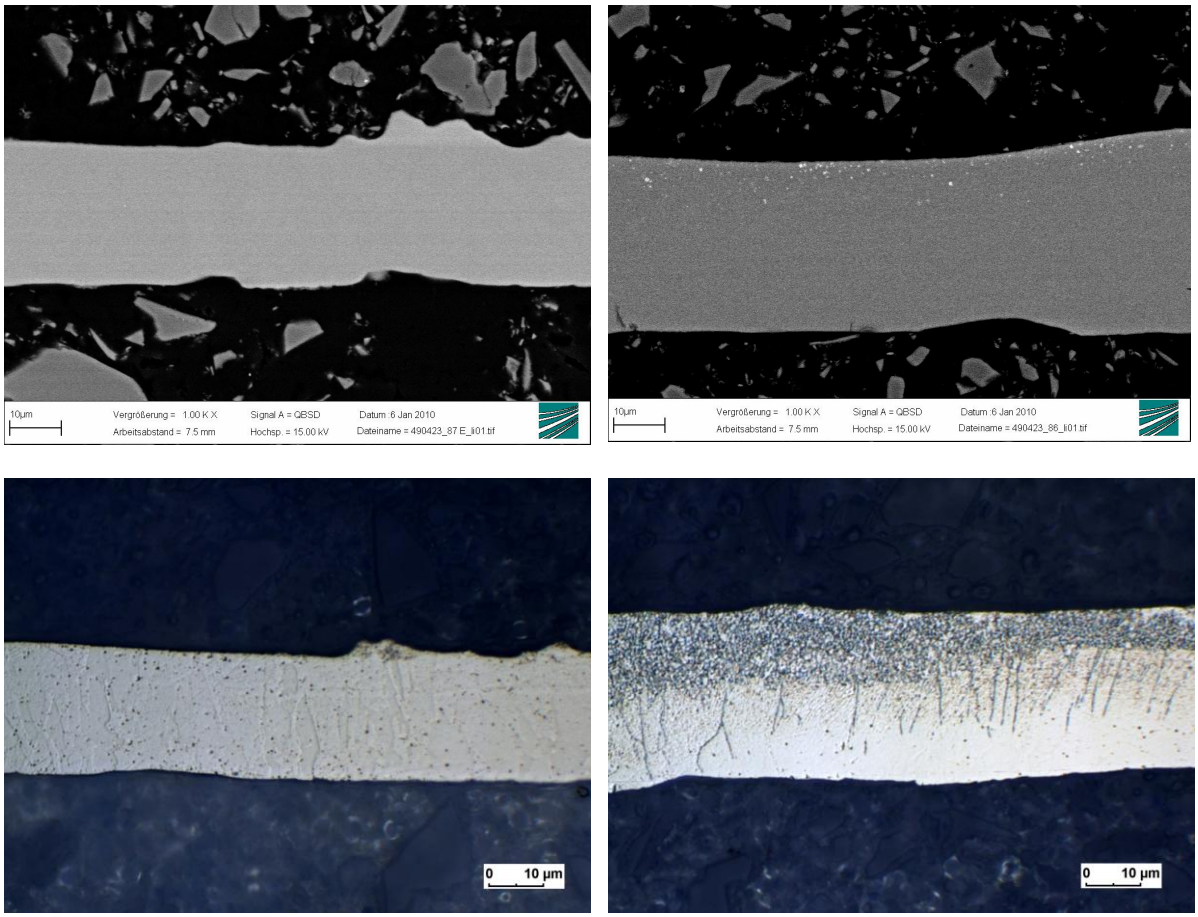

a) b)

Figure 3: Comparison of SEM image (top) to the etched optical micrographs of cross-sections (bottom) of different ribbon sections after rapid solidification with thickness of (a) 25 µm and (b) 35 µm.

Due to the demonstrated correlation between ribbon thickness and absolute microhardness reached after heat treatment, measurements “perpendicular“ to the ribbon direction followed. The lowest hardness of 148 HV on the upper and bottom side can be stated with the ribbon in figure 3a. For the lamellar microstructure on the wheel-side face in figure 3b 148 HV can be measured, too. In contrast, an higher hardness value of 165 HV is measurable on the air side face with the globular microstructure (figure 3b), which means a slower cooling rate, and therefore a lower forced dissolution of Sc and Zr. These differences in hardness indicate the necessity of low ribbon thickness and consequently high cooling rates during production. Thus only can achieve a complete dissolution of Sc and Zr, which leads to the required precipitations and explicitly increase in hardness at the following heat treatment. However, other investigations concerning quenching temperatures stated that for a complete suppression of $Al_3(Sc_{1-x}; Zr_x)$-precipitations during rapid quenching temperatures of about 1.400 °C are necessary. The authors suppose that at lower temperatures an arranged structure of Al, Sc und Zr in the molten metal exists. In order to that there are always Sc and Zr in solid solution but also $Al_3(Sc_{1-x}; Zr_x)$-precipitations in the rapidly solidified ribbon provable [10].

Both, the figures 4a and b illustrate a grain boundary running diagonally in a TEM image. The dark areas on the grain boundaries are stresses which cause electron deflexion. In the left image (a), there is no evidence of precipitated phases in the grains themselves. On the contrary, grey areas in (b) can be identified as precipitations after the heat treatment at 300 °C for 2 h. $Al_3(Sc_{1-x}; Zr_x)$-precipitations of 10-20 nm in size are visible.

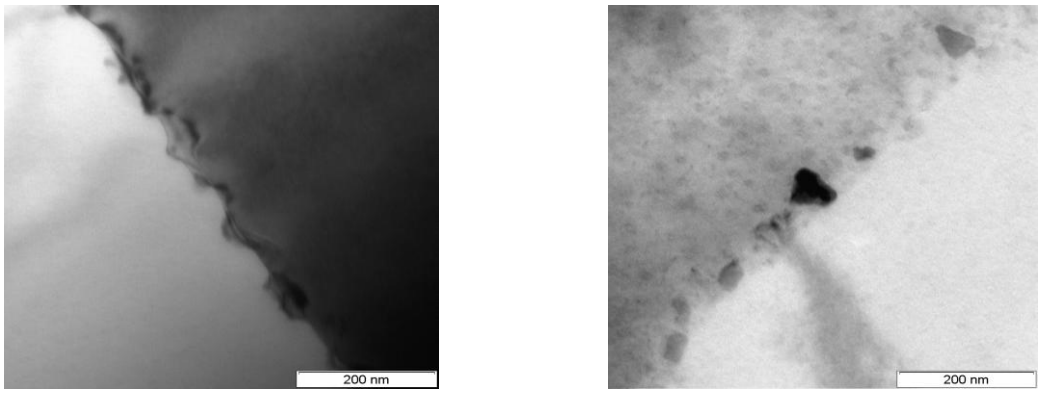

a) b)

Figure 4: TEM images of rapidly solidified (a) and heat treated structure at 300 °C for 2 h (b). Grey area in the grains (b) are $Al_3(Sc_{1-x}; Zr_x)$-precipitations.

In previous studies the rapidly solidified reference material was compacted by hot isostatic pressing (HIP) and an hardness of about 200 HV could be measured [3]. The HIP-process is often used for the compaction in the powder metallurgy. The SPS-compaction process is characterised by a very short cycle time, which suppress the material structure changes by long and high thermal stress. The compaction of rapidly solidified ribbons was carried out after their chopping by Spark Plasma Sintering into dense cylindrical blanks with 45 mm in diameter. All runs were executed in dynamic vacuum using two heating steps from room temperature to the desired sintering temperature, as can be seen in the diagram in figure 5. A first ramp up to 250 °C for some minutes was used for degassing the pre-compacted flakes and to decrease the hydrogen content from about 40 to 20 ppm [11, 12]. The resulting sintering temperature of 325 °C for 120 s was measured in the die. With an applied pressure of 180 MPa the relative density of the consolidated sample is about 99.7 % of theoretical density. Residual porosity can be seen in the cross-section in figure 6a. The lamellar structure (figure 6b) where no precipitations were analysed can be proven in many parts. Nevertheless, the measured microhardness in the blanks were between 160 und 175 HV which is an increase compared to the rapidly solidified starting material. The lower hardness of the SPS-compacted material in comparison to 200 HV of the HIP-ed material could mean a lower formation of precipitates. Although, butterfly-shaped $Al_3(Sc_{1-x},Zr_x)$-precipitations exist in individual ribbon areas (figure 6d). However, these occur only on one ribbon side, so that it can be assumed that they have already been formed on the upper side in the rapidly solidified ribbon before its compaction because of a locally insufficient cooling rate.

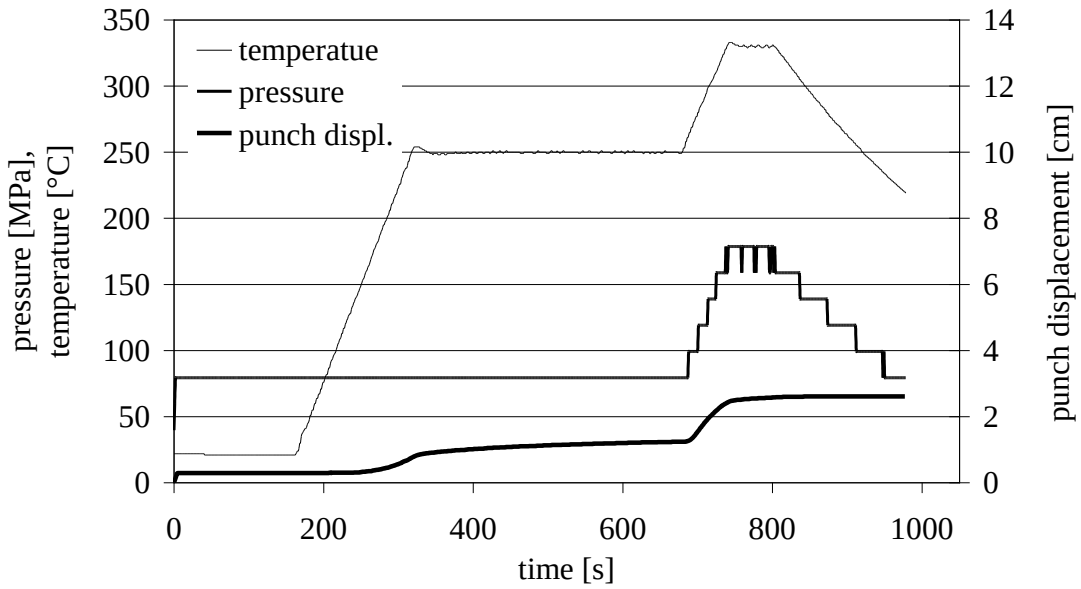

Figure 5: The used SPS -parameters, i.e. temperature-time-cycle during pre-compaction of the flakes.

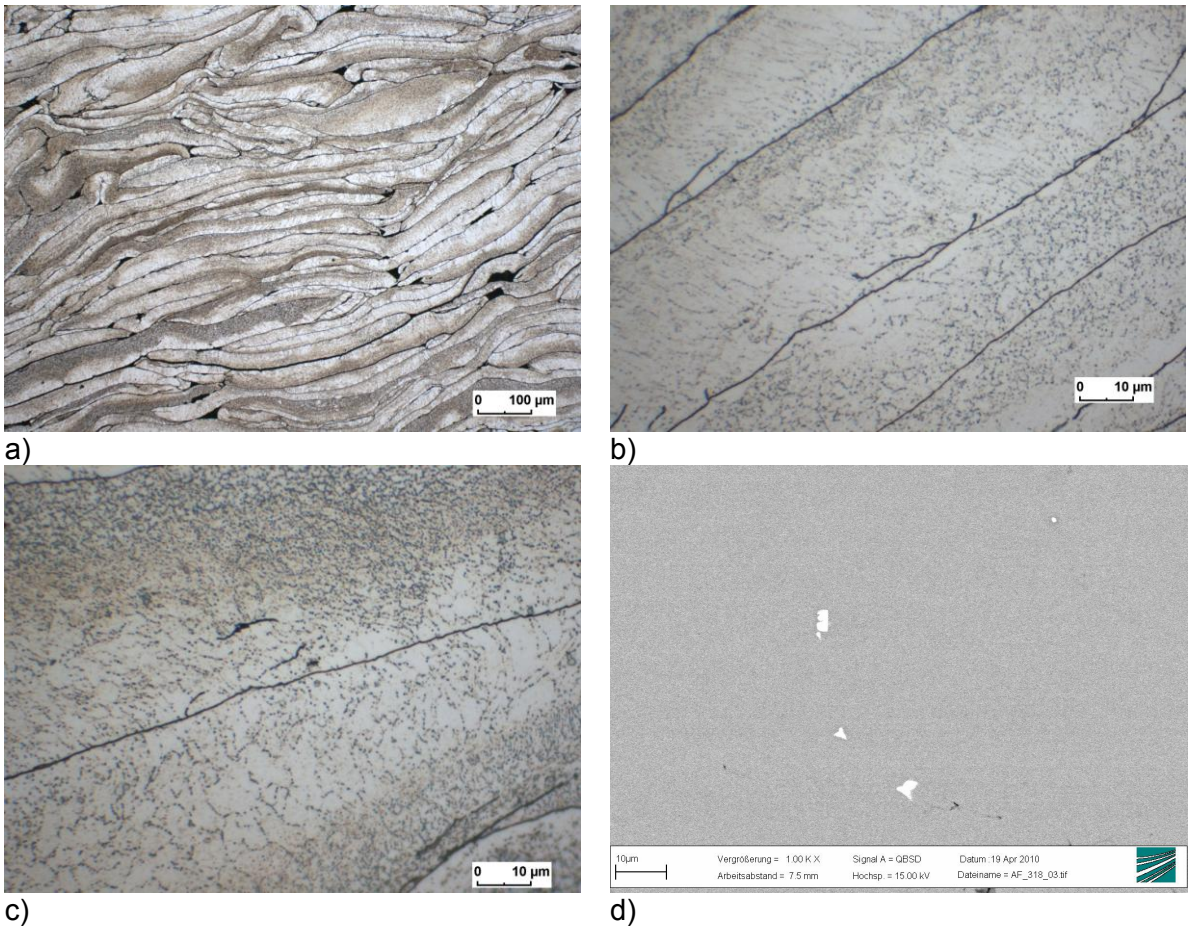

a) b)

c) d)

Figure 6: Optical micrographs of etched cross-sections of rapidly solidified and SPS-pre-compacted flakes (a) overview, (b) detail of lamellar microstructure, (c) lamellar-globular microstructure and (d) SEM image in backscattering mode showing butterfly-shaped $Al_3(Sc_{1-x},Zr_x)$-precipitations.

Summary and Conclusion

High cooling rates at melt spinning can cause the forced dissolution of higher Sc and Zr concentrations in aluminium compared to the conventional melting metallurgy. A successfully forced dissolution of the alloying elements leads to a reduced hardness of the rapidly solidified material. However, the formation of $Al_3(Sc_{1-x}; Zr_x)$-precipitations could not be suppressed completely during the melt-spinning of the Al Mg3.6Sc1.4Zr0.2Mn0.3 alloy. It seems that the necessary high cooling rates can only be achieved in parts of the ribbons with a thickness < 25 µm. During the following thermal treatments of processing the dissolved Sc in combination with Zr forms the $Al_3(Sc_{1-x}; Zr_x)$-phase which was verified by an increase of the hardness. The maximum hardness of 240 HV was only measured on very thin ribbons tempered at temperature of 300 °C and annealing times of 2 h. As the temperature increases, the particular maximum hardness emerge at an earlier stage. In comparison to hardness values of 200 HV (630 MPa) of previous studies with the reference material a slight improvement has been reached, which can result in a capability of 680 – 720 MPa UTS.

The pre-compaction of rapidly solidified flakes by SPS to nearly dense material with a limited formation of $Al_3(Sc_{1-x}; Zr_x)$-precipitation was shown. The SPS pre-compacted samples showed lower hardness values compared to the reference material produced by HIP. This preserved low hardness of the pre-compacts can cause a reduced resistance to the subsequent deformation, e.g. by hot extrusion. The temperature strain can be carried out in the above-mentioned parameter field, so that the maximum hardness exists in the material after the final hot forming. A further reduction of the hydrogen content can improve the weldability. There is some further optimization work necessary to manufacture the full capability of the material.

References

[1] F. Palm: Hypereutectic high strength AlMgSc profile material, Melt-spun Scalmalloy® - a new family of weldable and corrosion free Al alloys with 500 – 850 MPa strength, AeroMat, Seattle, 2006.

[2] F. Palm: Scalmalloy® = A unique high strength and corrosion insensitive AlMgScZr material concept. ICAA11, Aachen, 2008.

[3] F. Palm, R. Leuschner, T. Schubert: Scalmalloy® = A unique high strength AlMgSc type material solution prepares the path towards future eco-efficient aerospace applications. AeroMat, Dayton, 2009.

[4] M. Sugamata, J. Kaneko, H. Fujii, M. Kubota: Effect of Mg addition on the structures and mechanical properties of rapidly solidified Al-transition metal alloys. Materials Science Forum Vols. 331-337 (2000) 1157-1162.

[5] M.E. Drits, L.S. Toporova, Y.G. Bykov, et. al.: Metastable Al-Sc-phase diagram in Al-rich region. IAN SSSR, Metally, No. 1 (1983).

[6] V.I. Elagin, V.V. Zakharov, T.D. Rostova: Special features of recrystallization of Sc-bearing Al alloys, VILS, Moscow (1991) 114-129.

[7] L.S. Toropova, D.G. Eskin, M.L. Kharakterova, T.V. Dobatkina (Eds.): Advanced aluminium alloys containing scandium – structure and properties. Gordon and Breach science publishers, Amsterdam, 1998.

[8] V.V. Zakharov: Effect of Sc on the structure and properties of Al alloys. In Met. Sc. and Heat Treatment, Vol. 45 (2003) 246-253.

[9] J. Røyset, N. Ryum: Some comments on the misfit and coherency loss of Al_3Sc particles in Al–Sc alloys. Scripta Materialica 52 (2005) 1275-1279.

[10] A.L. Berezina et. al.: Phenomenon of the anomalous supersaturation in Al-Sc, Al-Mg-Sc alloys rapid quenchend from the liquid state. Eng. Mechanics, Vol. 11, No. 5 (2004) 393-397.

[11] K. Sastry: Compaction of complex aluminium alloy powders for preparing industrial components through field assisted sintering technology (FAST). Doctoral thesis (2006) Katholic University Leuven.

[12] T. Nagae, M. Yokota, M. Nose, S. Tomida, K. Otera, T. Kamiya, S. Saji: Microstructure and mechanical properties of gas atomized aluminium alloy powder compact densified by pulsed current pressure sintering process. Materials Trans., Vol. 43, No. 3 (2002) 537-543.